Three New Topics in Solid-Liquid Flow (TSE03P, TSE03Q)

Daniel D. Joseph
University of Minnesota, PI

Pushpendra Singh
NJIT, Co-PI

B. Project Summary

The projects proposed here are combined computational and experimental studies of three new problems of solid-liquid flows. The first problem is to obtain explicit formulas for the lift on particles in shear flows of pure fluids and slurries by correlating data from direct numerical simulation (DNS). The numerical studies to be undertaken look to the development of methods for interrogating the underlying mechanics of principles and correlations rather than to code development. The first problem is submitted for funding as a GOALI grant in collaboration with Barree and Associates, a consulting firm specializing in stimulation and well performance optimization. This collaboration follows our earlier GOALI grant in collaboration with STIM-LAB, a laboratory supported by a consortium of oil and oil service companies, which carries out experiments providing real data for correlations and modeling, which may be used for validating numerical experiments from DNS. Bob Barree Mike Conway (from STIM-LAB) and the PI's group have made good progress toward a proppant flow-back model and other software products addressing unsolved practical problems of the fracturing industry [7, 8].

The second problem is to study self-assembly and structure formation due to capillary attraction of floating particles by DNS and in experiments. Singh and Joseph [1] have presented the first numerical study by DNS of the dynamics of floating particles driven by capillary forces in the interface between two fluids when the contact angle is prescribed. These forces lead to capillary attraction of floating particles of the same wettability and to short range repulsion between particles of different wettability. The simulations are to be validated by experiments in studies aiming at precise description of effects not previously studied; for example, heavier than liquid cylinders with flat ends may be prevented from sinking by capillary forces at the sharp edge where the normal is not defined. The contact angle at the edge rotates so that a range of cylinders of different weights may be suspended.

The third problem is to study the surprising effects of small particles in moderate concentrations on the stresses generated in viscoelastic fluids. This problem is being submitted for ETS/NTE funding as a phase 1 proposal under sorting codes for transport processing (TSE03-P) and decontamination (TSE03-Q). The recent study of a particle laden tubeless siphon established that addition of small particles in concentrations of less than 12% by volume lead to very substantial increases in the pulling power of the tubeless siphon. It is as if the effective molecular weight of the mixture had been greatly increased; this property of the particle-laden tubeless siphon may allow contaminants to be cleaned remotely by suction devices. A program of experiments will be undertaken to determine the properties of the fluid and particles which most greatly enhance the pulling power of the particle laden tubeless siphon pointing to decontamination applications. The role of particles in enhancing extensional stresses is a virgin subject without a prior art. This subject can be attacked by comparing experiments with numerical studies building on codes for the DNS of particles in viscoelastic fluids developed under successive Grand Challenge and KDI-NSF grants led by the PI.

Potential impacts. The processing of data from DNS for correlations leading to explicit formulas has a potential for broad impact on computing infrastructure in which intelligent processing of huge amounts of data is an opportunity and challenge. The proposed studies of cleanup of particle-laden viscoelastic fluids have implications for homeland defense. Such mixtures could be spread on contaminated surfaces or surfaces covered with anthrax pores and the contaminants captures in the sticky mixture; the safe removal of trapped contaminants by sucking devices is a research goal of broad impact. For dangerous contaminants, in which even trace residues are a threat, the research will look to selecting fluid-solid (possibly chemically active) mixtures to neutralize rather than remove the residues.

Joseph [2] has published a web-based book *Interrogations of Direct Numerical Simulation of Solid-Liquid Flows* on *http://www.efluids.com/efluids/books/joseph.htm.* It is the first such book published on the web site, possibly on any web site. The new opportunity advanced by web-based publishing is updating without publisher

permission. The results of the proposed research will be disseminated in this as well as in more traditional ways. Web-based publishing has a very broad implication for the way scientific works are disseminated.

The PI's fluid mechanics laboratory has a tradition of involving large numbers of undergraduate students sponsored by REU supplements. Among seven graduate students working on projects related to this proposal, three are women.

D. Project Description

This project is to study three new problems of solid-liquid flows; these will be described in sequence after a review of relevant results form prior NSF support.

The ***results from prior NSF support*** most closely related to this proposal are from a GOALI award to the University of Minnesota and STIM-LAB on Direct Numerical Simulation of Slurry Transport Focussing on Engineering Correlations, NSF/CTS 0109079; Sept. 1, 2001 to Aug. 31, 2004 for $290,000. STIM-LAB is a research laboratory in Duncan, OK supported by a consortium of oil production and oil service companies interested in reservoir stimulation. The proposal was to develop and apply direct numerical simulation (DNS) to problems of slurry transport in general and to proppant transport into reservoir fractures in particular. We proposed to deliver a practical product to the fracturing industry in the form of (1) formulas for lift and drag on particles to be used by PC-based models of slurry transport and (2) correlations based on the processing of numerical experiments and real experiments using the same dimensionless parameters in log-log plots. Seven research papers [3, 4, 5, 6, 7, 8, 9] supported by the GOALI grant were or are to be published in 2002 and 2003; PDF files for the paper on power law correlations may be downloaded from Joseph's Power Law Archive[1].

Formulas for lift of single circular particles in a shear thinning 2D Poiseuille flow were generated by Wang and Joseph [3]. The proposed research seeks to generalize their 2D results to 3D and to extend computations to include drag and lift on a test particle in a swarm of many particles. Two papers developing correlations from experimental data obtained by STIM-LAB in Duncan, OK address the problem of proppant transport in fractured reservoirs and generalize to correlations for sediment transport [7, 8]. These papers introduce new features not seen before such as bi-power laws and rational fractions of power laws, which are explained in the project description. Mike Conway and Bob Barree from STIM-LAB are co-authors of the paper last mentioned; they developed a model of proppant flowback (see *Modeling of Proppant Flowback* 2002 at the Power Law Archive[1]), which is a central problem of the fracturing industry, based on correlations produced in our joint work. The occurrence of undesirable flowback into the well bore lengthens clean out time and increases disposal cost. The literature does not provide a clear understanding of proppant flowback causes or flowback prevention techniques.

The GOALI project was made possible by two successive NSF HPCC Grand Challenge awards ESC-95-2713, 10/01/95 to 09/30/98 and KDI/NCC award CIS-9873236, 9/15/98 to 8/30/01 that targeted the direct numerical simulation of solid-liquid flows. D. Joseph was PI on these grants and P. Singh was a senior investigator supported by subcontracts. Two types of codes to move particles in DNS were developed. One type of code uses a finite element method on an unstructured body-fitted mesh, together with an arbitrary Lagrangian-Eulerian (ALE) moving mesh technique to deal with the movement of particles. The ALE code is very accurate due to mesh adaptively but it requires remeshing after mesh distortion and the remeshing is essentially a serial and not parallel operation. The second type of code is set on a structured mesh and the particles are represented by a distribution of Lagrange multipliers (DLM). Both methods use a new combined weak formulation in which the fluid and particle equations of motion are combined into a single weak equation of motion from which the hydrodynamic forces and torques on the particles have been eliminated. Several different kinds of code have been developed and tried on a variety of applications. See the project web site *http://www.aem.umn.edu/Solid-Liquid_Flows*.

We proposed and implemented a strategy for treating collisions between particles which allows hydrodynamic forces to keep particles apart to within the tolerance of the mesh [4]. Formerly, we prevented collisions by invoking a force in a security zone to force nearly touching particles apart. This force does not belong to the problem's description. Smooth particles should not collide, there is always a liquid film if we do not provide for film rupture, and the repulsive lubrication forces get larger and larger as the film gets smaller. The solution to this problem implemented in [4] is to activate artificial forces in a security zone inside the particle. Artificial forces are activated

[1] See the Power Law Archive at *http://www.aem.umn.edu/people/faculty/joseph/PL-correlations/*

only in the artificial overlap situation. When the particles are close but not overlapping, only hydrodynamic forces will act. This strategy allows particles at rest to close pack.

Prior literature

There are a number of numerical packages, other than those mentioned above, which could be used to generate correlations. The methods of Stokesian dynamics [10] can be recommended for problems in which inertia is absent. Hofler, Muller, Schwarzer and Wachmann 1999 [11] introduced two approximate ALE simulation methods. In one method, the particle surface is discretized in a grid topology; spheres are polygons on flat places between nodes. In the second method a volume force term is introduced to emulate rigid body; this method is similar to the powerful force coupling methods introduced by Maxey and Patel [12]. Hofler *et al* [11] calculated sedimentation of 65,000 spheres at very small Reynolds numbers. Johnson and Tezduyar [13] used a fully resolved DNS/ALE method to compute sedimentation of 1000 spheres at Reynolds numbers not larger than 10. Recently improvements in the DLM method by Yu, Tanner and Phen-Thien [14] and Yu, Phen-Thien, Fan and Tanner [15] should be effective for developing correlations in the spirit of the proposal. The problem of particulates in turbulent flow has been considered by a few authors [16, 17, 18]; these approaches use point particle approximations because fully resolved computations in turbulent flow are not presently possible.

I. Method of correlations (this problem is being submitted for funding under GOALI, partnering with Barree & Associates for studies of proppant transport in fractured reservoirs.)

There is a ubiquitous but not well understood tendency for flowing dispersions to follow self-similar rules described by power laws. This tendency can be exploited to generate analytical formulas by correlating the data from real or numerical experiments. Although this method forms the basis of many industrial applications, it has received a bad name because it is perceived as empirical, not fundamental. Used with care, however, and with attention to the underlying physics it can deliver outstanding results.

Advances in computer hardware and software have greatly facilitated the construction of accurate and useful correlations. We have been developing and promoting procedures to take advantage of the new possibilities. Given a set of data from simulations or experiments, such as transport of fluidized proppants in slots (modeling proppant transport in fractured oil or gas reservoirs) or gas-liquid flows in horizontal pipes, we proceed as follows.

First, list the relevant variables—material properties, process variables, and measured data—in the columns of a spreadsheet. Of course we must first understand the system well enough to know what might be relevant.

Second, identify the controlling dimensionless parameters. Correlations of maximum generality are formulated in terms of these. The determination of the best dimensionless parameters for multiphase flows is highly nontrivial and requires experience. Conventional dimensional analysis has not been particularly useful—perhaps because the dynamics of multiphase flow is controlled by the distribution and interaction of the phases, and these are functionals of the solution and therefore cannot be specified in advance. Instead we focus on the dimensionless forms of the governing equations for solid-liquid flow.

For the motion of circular particles of diameter d in a 2D Poiseuille flow in a periodic channel of height w, for example, the dimensionless form of the governing equations is [19]

$$\nabla\cdot\mathbf{u}=0,\qquad R\left(\frac{\partial\mathbf{u}}{\partial t}+\mathbf{u}\cdot\nabla\mathbf{u}\right)=-\nabla p+2\frac{d}{w}\mathbf{e}_x+\nabla^2\mathbf{u} \tag{1}$$

for the fluid velocity $\mathbf{u}$ and pressure p, and

$$\frac{\rho_{\mathrm{p}}}{\rho_{\mathrm{f}}}R\frac{d\mathbf{U}_{\mathrm{p}}}{dt}=-\frac{R_{\mathrm{G}}}{R}\mathbf{e}_y+2\frac{d}{w}\mathbf{e}_x+\frac{4}{\pi}\int_0^{2\pi}\left(-p\mathbf{n}+2\mathbf{D}[\mathbf{u}]\cdot\mathbf{n}\right)d\theta\,, \tag{2}$$

$$\frac{\rho_{\mathrm{p}}}{\rho_{\mathrm{f}}}R\frac{d\boldsymbol{\Omega}_{\mathrm{p}}}{dt}=\frac{32}{\pi}\int_0^{2\pi}\left(\mathbf{x}-\mathbf{X}\right)\wedge\left(-p\mathbf{n}+2\mathbf{D}[\mathbf{u}]\cdot\mathbf{n}\right)d\theta \tag{3}$$

for the velocity $\mathbf{U}_{\mathrm{p}}$ and angular velocity $\boldsymbol{\Omega}_{\mathrm{p}}$ of the particle. The flow is determined by the four dimensionless parameters

$$\frac{\rho_p}{\rho_f}, \quad \frac{2d}{w}, \quad R = \frac{\rho_f \dot{\gamma}_w d^2}{\eta}, \quad R_G = \frac{\rho_f (\rho_p - \rho_f)}{\eta^2} g d^3$$

where $\dot{\gamma}_w$ is the wall shear rate and η is the viscosity. (The density ratio does not enter in problems of steady flow because the accelerations vanish.) The most important parameters are the shear Reynolds number R and the gravity Reynolds number R_G.

Third, correlate the data to power-law or bi-power-law formulas. For example, Patankar, Huang, Ko, and Joseph [20] used DNS on (1)—(3) to study the lift-off of a heavier-than-liquid circular particle from the bottom of the channel in a 2D Poiseuille flow. They found that there is a critical value R_c of R for lift-off. When $R < R_c$ the particle slides and rolls along the bottom of the channel; when $R > R_c$ it lifts off and rises to a height where the lift force balances its buoyant weight, after which it moves along at a constant height and speed. Heavier particles are harder to lift off. Patankar *et al.* plotted the critical Reynolds number $R = R_c$ against R_G from about 25 DNS experiments on a log-log plot. They found that the data lie very close to the straight line corresponding to the power law

$$R_G = aR^n, \qquad a = 2.36, \qquad n = 1.39. \tag{4}$$

Similar correlations could be found for various dimensionless quantities at equilibrium, such as the equilibrium height, and the particle slip velocity U_s and slip angular velocity Ω_s. (The latter two quantities are defined as the *differences* between the velocity and angular velocity of the particle and those of the undisturbed Poiseuille flow at the same position.)

Another example of a power-law correlation is the famous Richardson-Zaki formula [21]

$$\frac{V(\phi)}{V(0)} = (1-\phi)^{n(R)} \tag{5}$$

for the fluidization velocity $V(\phi)$ of a suspension of particles of volume fraction ϕ. The exponent $n(R)$ was found to depend on the Reynolds number $R = \rho_f V(0) d/\eta$. For small particles, $n = 4.65$ when $R < 1$, $n = 4.45/R$ when $1 < R < 500$, and $n = 2.39$ when $500 < R < 7000$. Correlation (5) was obtained by plotting the results of many experiments in a log-log plot. Pan, Joseph, Bai, Glowinski, and Sarin [5] found $n = 2.33$ (instead of 2.39) by plotting the results of a 3D simulation of the fluidization of 1204 spheres for $R = O(1000)$ in log-log plots.

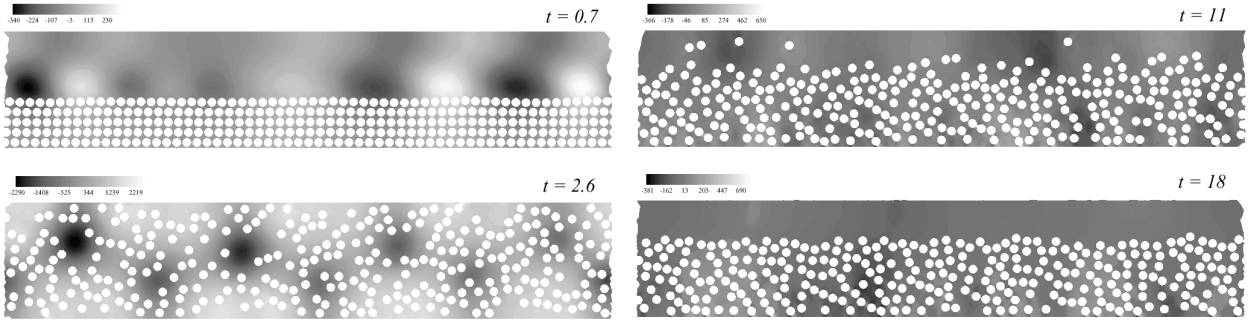

Figure 1. Snapshots of the fluidization by lift of 300 circular particles of density $\rho_p = 1.01$ gm/cm^3 when $\eta = 1$ poise ($R = 1800$, $R_G = 981$). The flow is from left to right. The gray scale gives the pressure intensity with dark representing low pressure. At early times particles are wedged out of the top layer by high pressure at the front and low pressure at the back of each particle in the top row. The vertical stratification of pressure at early times develops into a "periodic" horizontal stratification—a propagating pressure wave. The inflated bed at t = 2.6 *eventually settles down, with rather tightly packed particles at the bottom and fluidized particles on top.*

Correlations like (4) arise in relatively simple situations in which only two dimensionless parameters are active and the flow regime is self-similar. However even in situations where more than two dimensionless parameters are active we can obtain correlations of this type by processing the parameters two at a time, leading to *bi-power laws*. The selection of these parameters is not routine. For example Patankar, Ko, Choi, and Joseph [19] used DNS to study a slurry of 300 heavy circular particles in a 2D Poiseuille flow (see figure 1). They found that the equilibrium height of the bed increases—i.e., ϕ decreases—as R increases. Using log-log plots, they obtained a power law like (4) for each value of ϕ. Similarly they found that the prefactor $a(\phi)$ has a power-law dependence on ϕ, for fixed R and R_G. Combining these results they obtained the bi-power law

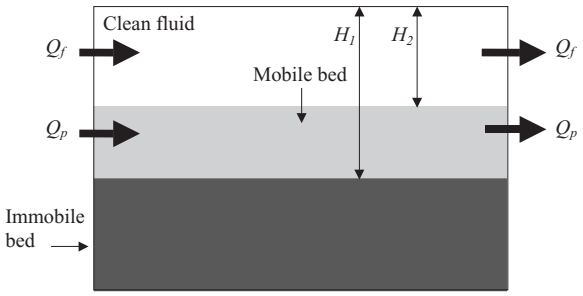

Figure 2. Proppant transport experiment.

$$R_G = 3.27 \times 10^{-4} (1 - \phi)^{-9.05} R^{1.249}, \tag{6}$$

which could be called a Richardson-Zaki correlation for fluidization by lift.

When considering correlations of the form (4) when other variables like ϕ in (6) are active, it is in general necessary to process the exponent n for correlations in terms of the other active parameters. In [7] and [8] for example, the investigators examine the data from 140 proppant transport experiments performed at STIM-LAB, in which 6 different sands were pumped through a slot of width $W = 7.95$ mm (see figure 2). They correlated the dimensionless parameters H_1/W and H_2/W (representing the heights of the immobile and mobile beds) with the gravity Reynolds number R_G, the fluid and particle Reynolds numbers $R_f = \rho_f Q_f/(W\eta)$ and $R_p = \rho_p Q_p/(W\eta)$, and the dimensionless viscosity $\lambda = \eta/(\rho_f W^{3/2} g^{1/2})$, where Q_f and Q_p are the volume flow rates of the fluid and proppant, obtaining

$$\frac{H_1}{W} = \left(-2.30\times10^{-4}\ln R_G + 2.92\times10^{-3}\right) R_f^{1.2-1.26\times10^{-3}\lambda^{-0.428}(15.2-\ln R_G)} R_p^{-0.0172\ln R_G - 0.120}, \tag{7}$$

$$\frac{H_2}{W} = \left(-1.15\times10^{-4}\ln R_G + 1.33\times10^{-3}\right) R_f^{1.2-1.30\times10^{-6}\lambda^{-1.28}(11.67-\ln R_G)} R_p^{-7.16\times10^{-3}\ln R_G - 0.304]}. \tag{8}$$

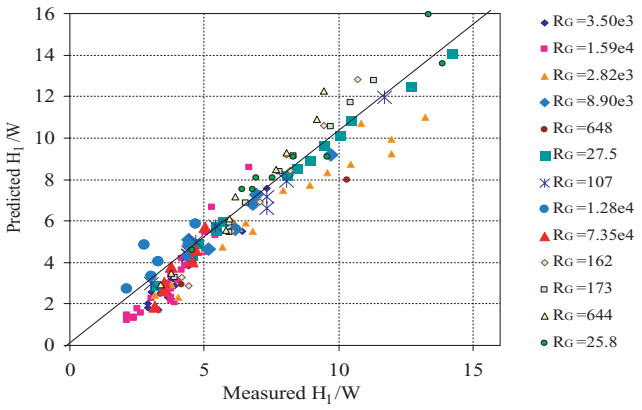

Figure 3. The values of H_1/W *predicted by (7) vs. the experimentally measured values for different sands.*

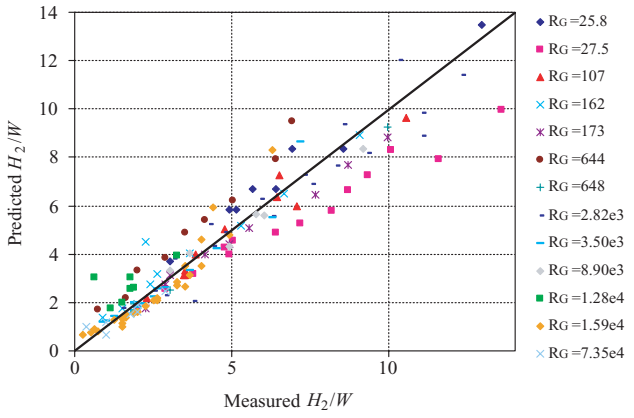

Figure 4. The values of H_2/W *predicted by (8) vs. the experimentally measured values for different sands.*

These explicit and predictive correlations for proppant transport are bi-power laws in R_f and R_p, with exponents and prefactors which are log laws in R_G and power laws in λ.

In figures 3 and 4 the experimental values of H_1/W and H_2/W are plotted against the values predicted by (7) and (8). Plots of this type should always be made to check the accuracy of the correlations.

Lift on Particles in Shear Flows

We propose to develop explicit formulas for the lift on a single particle in shear flows of pure fluids and slurries in 3D by correlating the data generated by DNS with power-law formulas. The simulation tools for this effort are already in place and are not a focus of the proposed research. Instead the aim is to interrogate the data in order to extract information in a form optimal for applications. The primary interrogation tool is the method of correlations.

Joseph and Ocando [6] used DNS to study how the lift force L on a circular particle of diameter d in a 2D Poiseuille flow of a Newtonian fluid in a horizontal channel depends on its height y_p. Using constrained simulations in which y_p is held constant and the particle velocity U_p and angular velocity Ω_p are allowed to evolve to steady state, they generated plots of L against y_p for several values of the shear Reynolds number R between 10 and 80. The case R = 20 is shown in figure 5. The curve has two stable and two unstable branches, separated by three turning points.

Figure 5. Lift vs. y_p *for* R = *20 for steady forward motion of a circular particle in 2D Poiseuille flow. The equilibrium points are the values of* y_p *at which the lift balances the buoyant weight. The horizontal line shown corresponds to* $\rho_p = 1.01\ \rho_f$*; there are two stable equilibrium points and one unstable. The curve is anti-symmetric with respect to the center of the channel; the graph shows that a region near the center is unstable [6].*

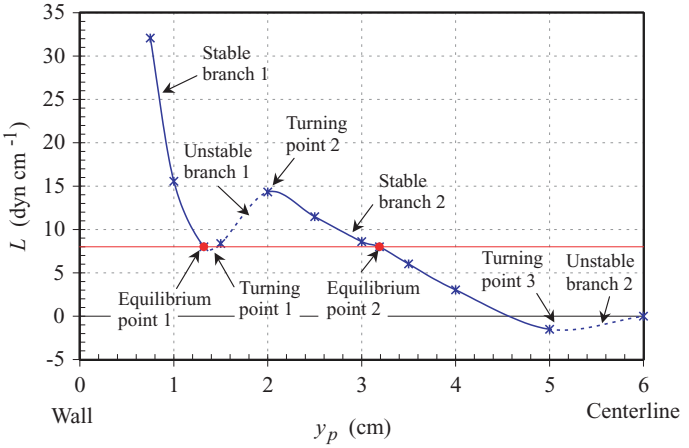

If $R > R_c$ a *free* particle of density ρ_p will migrate laterally, adjusting y_p, U_p, and Ω_p until equilibrium is attained—i.e., until L exactly equals the buoyant weight $(\rho_p - \rho_f)g\pi d^2/4$. The stable equilibrium height(s) y_e can be identified as the values of y_p at which the horizontal line $L = (\rho_p - \rho_f)g\pi d^2/4$ intersects the *stable* branches of the L vs. y_p curve. If $\rho_p - \rho_f$ is 0 (neutral buoyancy) or is relatively small—or very large—there is only one stable equilibrium height. For some intermediate densities, however, there are two stable equilibrium heights (and one unstable one). Joseph and Ocando [6] found that no matter where in the channel the particle starts, it migrates to one of the stable equilibrium heights. At equilibrium, the *slip velocity* $U_s = U_p - U_f$ is always slightly negative, and the *slip angular velocity* $\Omega_s = \Omega_p - \Omega_f$ slightly positive, where U_f and $\Omega_f = -\dot{\gamma}/2$ are the velocity and angular velocity of the undisturbed Poiseuille flow at the position of the particle and $\dot{\gamma}$ is the local shear rate. Both quantities are, however, quite small.

An analytical formula for the lift force L may be constructed by analogy with the classical lift formula $L = \rho U\Gamma$ of aerodynamics. As detailed in [6], the proper analogs of U and Γ in the present context are U_s and the *slip angular velocity discrepancy* $\Gamma_s = \Omega_s - \Omega_{se}$, where Ω_{se} is the slip angular velocity at equilibrium, leading to the formula

$$L = CU_s\Gamma_s \tag{9}$$

for the lift on a neutrally buoyant circular particle. Joseph and Ocando found that $\Gamma_s > 0$ when $y_p < y_e$, and $\Gamma_s < 0$ when $y_p > y_e$, and thus that the predicted lift changes sign across the equilibrium position, as it must.

Wang and Joseph [3] carried out constrained simulations of the type described above to compute L, U_s, and Ω_s for values of y_p on the stable branches of the L vs. y_p curve, for Reynolds numbers R from 20 to 160, and used the method of correlations to express the prefactor C in (9) as a power law in R. (They carried out the same kind of analysis for shear-thinning fluids.) The correlations, expressed in terms of the dimensionless parameters

$$\Lambda(y_p, R) = \frac{4\rho_f dL(y_p, R)}{\pi\eta^2}, \qquad F(y_p, R) = \frac{\rho_f^2 U_s(y_p, R)\left(\Omega_s(y_p, R) - \Omega_{se}(R)\right) d^3}{\eta^2},$$

(where $\Omega_{se}(R)$ is the unique slip angular velocity discrepancy of a neutrally buoyant particle) are

$$\Lambda(y_p,R) = 5.34\, R^{\,0.428}\, F(y_p,R)^{\,0.0007R+0.386}$$

on the stable branch near the wall, and

$$\Lambda(y_p,R) = 232.5\, R^{\,-0.515}\, F(y_p,R)$$

on the stable branch near the center. The latter equation may be written as

$$L(y_p,R) = 182.6\, R^{-0.515}\, \rho_f\, U_s(y_p,R)\, \left(\Omega_s(y_p,R) - \Omega_{se}(R)\right)\, d^2, \tag{10}$$

completing (9). Recently [3] we have obtained correlations of the form

$$U_s(y_p, R) = a(y_p)R^{m(y_p)}, \qquad \Omega_s(y_p, R) = b(y_p)R^{p(y_p)}.$$

The prefactors $a(y_p)$ and $b(y_p)$ can be fit to splines, which will make (10) completely explicit.

We are proposing to develop explicit lift formulas like (10) in 3D. To validate the 3D formulas we are planning to perform simulations using Howard Hu's ALE code, Pan and Glowinski's DLM code, and the DLM code recently developed for this problem by P. Singh. The 3D lift results will also be compared with experiments. It should also be possible to derive lift formulas for particles in slurries. In 2D we would identify a test particle in a fully expanded bed and carry out a constrained simulation in which its y position is held fixed but its velocity and angular velocity are allowed to evolve to a pseudo steady state.

II. Capillary attraction of floating particles

It is well known that the small tea leaves floating on the tea surface collect near the cup wall which is due to the formation of meniscus that rises near the wall and results in a net capillary force towards the wall. The meniscus rises near the wall because the water wets or likes the cup. If, on the other hand, the liquid does not like the cup, i.e., the meniscus falls near the cup wall, floating small particles tend to move away from the wall and towards the center of the cup. Similarly, the deformation of liquid-liquid interfaces due to floating light particles, or due to trapped heavy particles, gives rise to capillary forces on the particles which cause them to cluster, as can be seen in figure 6. The clustering of particles on interfaces is important because it modifies the interfacial properties of the two-phase system and has been used in many flotation based extraction and separation processes [22]. More recently, this effect has been used for the self-assembly of submicron sized particles on two-liquid interfaces (see [23, 24, 25] and references therein).

The motion of tea leaves along the interface, in the above example, is entirely due to the deformation of the meniscus near the cup wall. The clustering of particles, on the other hand, is a consequence of the interface deformation caused by neighboring particles. Specifically, when two heavy particles, hydrophobic with respect to the lower liquid, are sufficiently close to each other the deformed interface shape around the particles is not symmetric about the vertical passing through their respective centers, as the interface height between the particles is lowered due to the interfacial force which acts downwards (see figure 7a). If, on the other hand, the particles are less dense than the lower liquid and hydrophilic with respect to it, the interface height between the particles is raised due to the action of interfacial force (see figure 7b). In both of these cases, the lateral component of interfacial tension is attractive which causes the spheres to move toward each other. But, when one particle is hydrophilic and the other is hydrophobic with respect to the lower liquid, the lateral force is repulsive which causes them to move away from each other.

A finite element code based on the level set [26] and distributed Lagrange multiplier (DLM) method [27] is developed for simulating the motion of rigid spherical particles on two-fluid interfaces. The interface position is tracked using a level set function.

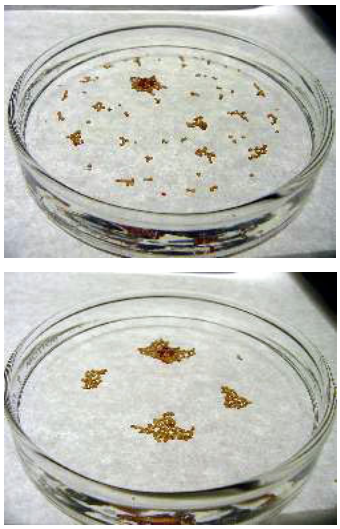

Figure 6. Sand in 1% aqueous Polyox solution.

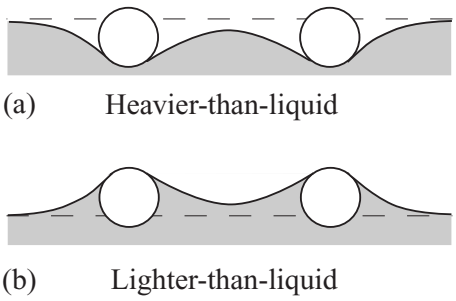

Figure 7. Spherical particles in water, (a) heavier-than-water hydrophobic particles. The meniscus between the particles is below the undisturbed level. Assuming that the contact angle remains fixed, the horizontal component of capillary force moves them toward each other. (b) Lighter-than-water hydrophilic particles will rise into the elevated section of the meniscus and come together.

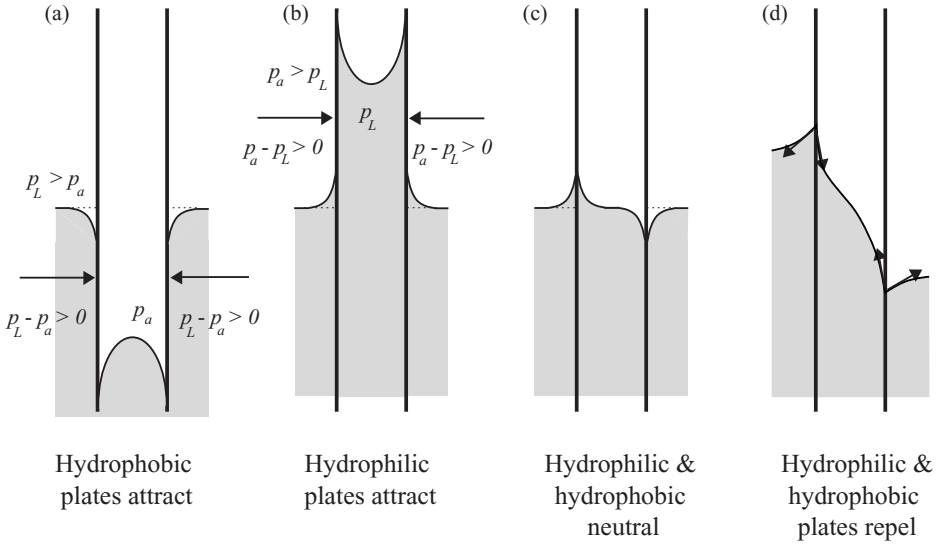

Figure 8. [After 28]. Horizontal forces associated with the fall (a) of liquid between hydrophobic plates and the rise (b) of liquid between hydrophilic plates. In (c) and (d) one plate is hydrophilic and the other hydrophobic. The contact angles on both sides of a plate are the same and the tension σ is constant. They argue that the net horizontal force due to σ can be calculated at flat places; so that there is no net horizontal component of the tension. In (a) and (b) the pressures are such that they push the plates together; there is no net attractive force in (c). In (d) the plates are so close that there is no flat place, and the horizontal projection $\sigma \sin \alpha$ of the interface midway between the plates is smaller than the horizontal component outside the plates and the plates are pulled apart; they repel. They note that "…small bodies, such as straw or pieces of cork, floating on the surface of a liquid often attract each other in clusters; this occurs when the bodies are all wet by the liquid and also when none of them is wet; if one body is wet and one is not wet, they repel each other."

The contact angle of the interface, which is fixed by the Young-Dupré equation, is maintained in the simulation by extending the level set into the particle. The particle can be said to move in a *constrained motion in which the contact angle is fixed and the contact line moves.*

Floating particles with sharp edges

It is well known, but not well understood that liquid-air-solid interfaces tend to locate on sharp edges and corners; heavy objects with sharp edges can be suspended in a free surface. Gibbs 1906 [29] derived a purely

geometric extension of the Young-Dupré equation which determines the equilibrium contact angle. The extension can be written as

$$\theta_0 < \theta < (180° - \phi) + \theta_0 \tag{11}$$

where θ_0 is the equilibrium contact angle, ϕ is the angle subtended by the two surfaces forming the solid wedge and θ is the measured contact angle on the sharp edge which is not determined by equilibrium thermodynamics and is not uniquely determined by (11). The validity of (11) was tested by Oliver, Hu and Mason 1996 [30] in experiments in which sessile drops resting on the flat end of a cylinder were attached at a sharp edge. Equation (11) was confirmed using a sapphire disk with a 90° edge and, to a lesser degree using aluminum disks with edges subtending a range of angles.

Here we show that a heavier-than-liquid cylinder with flat ends sinks to a stable floating position in which the sharp edge is attached to the interface. The weight of the cylinder can be changed by inserting ball bearings in a cone cavity centrally cut in the top of the cylinder. The cylinder will float in this manner even as the weight is increased with the caveat that the contact angle adjusts as the weight is added in such a way as to increase the vertical component of the interfacial force. The contact angle at the sharp edge is determined by a static force balance. At a sharp edge the contact line rather than the contact angle is fixed.

Vertical force balance

A cartoon defining the quantities which enter into the vertical force balance is shown in figure 9.

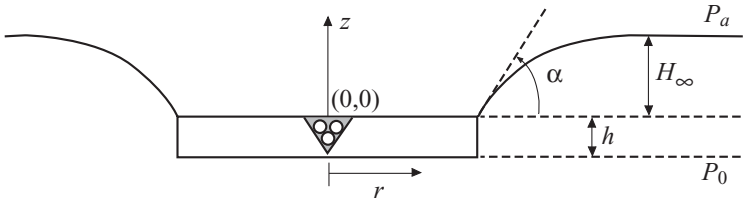

Figure 9. Force balance for a heavier than liquid cylinder hanging from a flat edge. The capillary force is given by $F_c = 2\pi R\sigma \sin\alpha$ *where* σ *is the interfacial tension.*

The weight mg of the cylinder is balanced by the sum of the capillary force $F_c=2\pi R\sigma\sin\alpha$, and the net pressure force $(P_0 - P_a)\pi R^2$, where $P_0 = P_a + \rho g(h + H_\infty)$; that is

$$2\pi R\sigma \sin\alpha + \pi R^2 H_\infty \rho g = mg - \pi R^2 h\rho g = (m - \rho V)g, \tag{12}$$

where $V=\pi R^2 h$ is the volume of the cylinder.

The shape of the interface $z = H(r)$ in figure 9 is determined by the balance between the pressure drop $\rho g[H(r) - H_\infty]$ across the interface and the surface tension σ times twice the mean surface curvature. In cylindrical coordinates this is expressed as

$$\rho g\left[H(r) - H_\infty\right] = \frac{\sigma}{r}\left[\frac{rH'(r)}{\sqrt{1 + H'(r)^2}}\right]', \tag{13}$$

where $r = 0$ and $z = 0$ are the axis and upper surface of the cylinder, respectively. The boundary conditions for this equation are (12), which can be written as

$$2\pi R\sigma \frac{H'(R)}{\sqrt{1 + H'(R)^2}} + \pi R^2 \rho g H_\infty = (m - \rho V)g, \tag{14}$$

and

$$\lim_{r\to\infty} r\,H'(r) = 0\,. \tag{15}$$

Equations (13) – (15) are to be solved together with the condition $\lim_{r\to\infty} H(r) = H_\infty$, which defines H_∞.

The values of α and H_∞ may be determined as functionals of the solution using (12) together with

$$\rho g \int_R^\infty [H_\infty - H(r)]\, r dr = \sigma R \sin\alpha\,, \tag{16}$$

which follows from (13) and (15). For example, if *H(r)* were the circular arc $H = H_\infty \sin\theta$, $r = R + H_\infty(1-\cos\theta)$, $0 \le \theta \le \pi/2$, (16) would become

$$\frac{\sigma R}{\rho g}\sin\alpha = \int_R^\infty [H_\infty - H(r)]\, r dr = \int_0^{\pi/2} H_\infty^2 (1-\sin\theta)(R + H_\infty[1-\cos\theta])\sin\theta d\theta = 0.2146 R H_\infty^2 + 0.0479 H_\infty^3\,.$$

Together with (12), this determines α and H_∞.

Experiment:

We used a 3.38g Teflon cylinder with a cone cut in the center. 0.25g steel beads were put in the cone to change the weight. The radius, height and volume of the cylinder are [1.27 cm, 0.495 cm, 2.51cc]. The angle α and the depression height H_∞ are measured using a video camera. Measurements are taken at several azimuthal positions and the average values of α and H_∞ are recorded. Inserting the measured parameters into the force balance equation (12), we can compute the residual

$$e = mg - 2\pi R\sigma \sin\alpha - V\rho g - H_\infty \pi R^2 \rho g \tag{17}$$

which exhibits the accuracy of our experiments. The ratio between *e* and *mg* is also computed. The surface tension coefficient σ is taken as 46 dyn/cm. The experimental data for five weights are listed in the following table.

***m*(g)**	3.38	3.63	3.88	4.13	4.38
α (degree)	28.4	37.8	43.0	51.7	71.1
H_∞(cm)	0.130	0.176	0.206	0.255	0.302
$2\pi R\sigma \sin\alpha$	174.8	224.7	250.3	288.3	347.2
$\rho g H_\infty \pi R^2$	644.7	873.9	1025.5	1269.9	1502.9
***e*(cm.g/s^2)**	34.3	0.4251	68.5	31.4	-15.4
$\lvert e\rvert$/mg	1.03%	0.01%	1.8%	0.77%	0.36%

Table 1. Quantities entering into the force balance equation (12). The residual e *computed by (17) exhibits the accuracy of our experiments.*

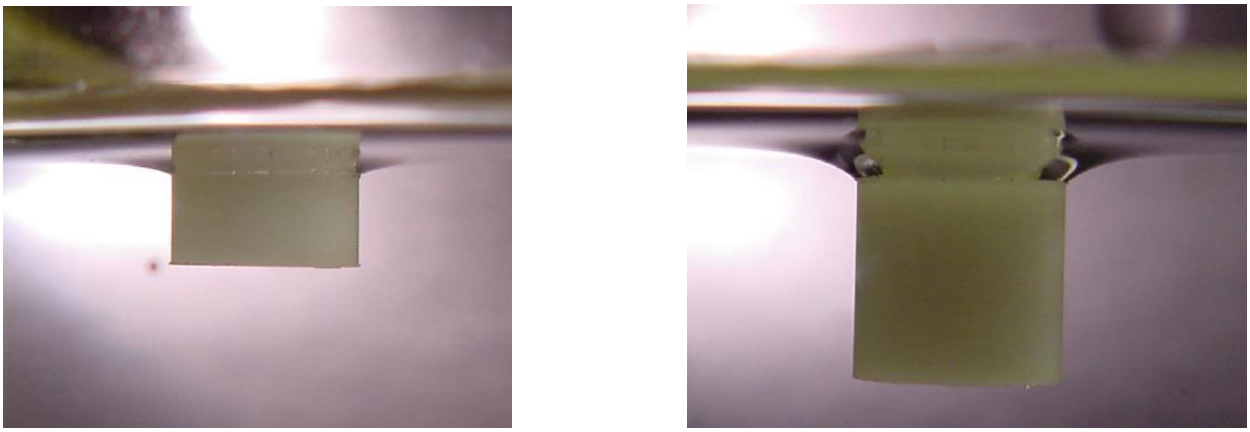

(a) (b)

Figure 10. Two photos of floating Teflon cylinders of density ρ_s=1.4g/cc held at the contact line in water of density ρ_f=1g/cc. Both cylinders have a diameter of 0.8 cm; the height from the bottom of the cylinder to the contact line is 0.4cm in (a) and 0.8 cm in (b). The contact angle in (b) is larger than that in (a) in order to satisfy the

force balance. What appears to be part of the cylinder projecting above the contact line is actually just a reflection in the surface of the water.

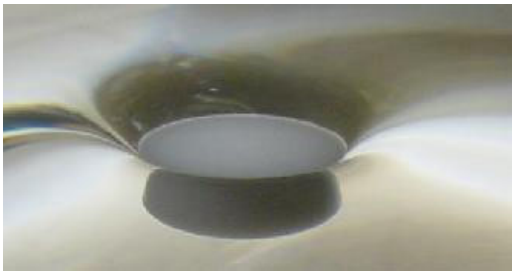

(a)

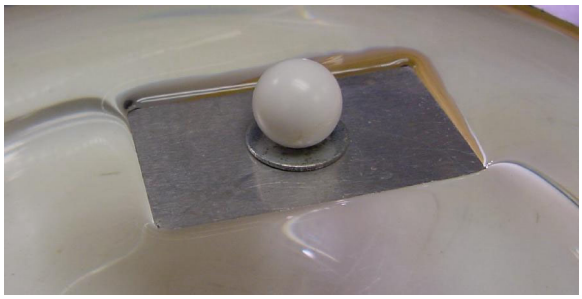

(b)

Figure 11. (a) The meniscus for a Teflon cylinder of density ρ_s=1.4g/cc hanging from a flat edge in water. (b) An aluminum plate can float in water hanging from the sharp edge; when weighted by a Teflon ball , the plate can still float but sinks into a deeper depression in water.

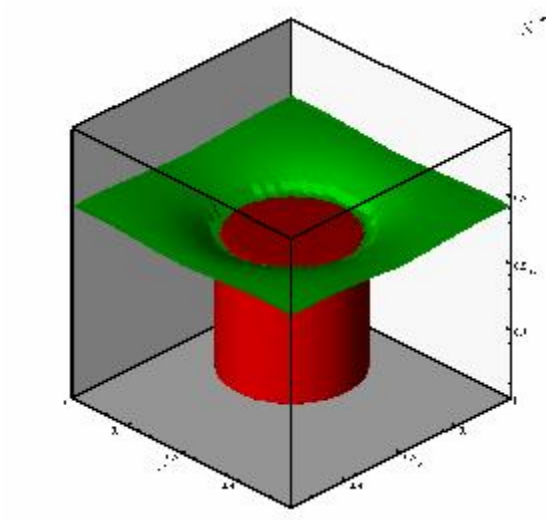

Figure 12. Floating cylinder held at the contact line from direct numerical simulation using DLM for the solid and level sets for the meniscus. The contact line is prescribed to attach to the sharp edge and the contact angle adjusts to accommodate the force balance. The numerical package allows for lateral motion under the prescribed contact line constraint. This picture can be compared with figure 10(b) in which a cylinder of density 1.4g/cc, diameter 0.8 cm and height 0.8 cm is suspended in water of density 1.0 g/cc at the contact line.

Projects: The projects on floating particles with sharp edges we propose to do are:

- Carry out experiments on capillary attraction of particles hanging in fluids at sharp edges.
- Carry out studies of particles with sharp edges in the interface between two liquids.
- Carry out experiments on the orientations of polygonal particles with flat faces and sharp edges.
- Solve equations (13) – (15) for H_∞ and α and compare the results with experiments.
- Develop a numerical code for computing lateral motions due to capillarity of heavier than liquid particles hanging in a liquid at sharp edges. The code we have developed computes the motion of smooth floating particles with the contact fluid fixed; the contact line must move. In the case of sharp edges, the contact line is fixed on the edge and the contact angle must change.

III. Effects of particles on extensional stresses (Particle-laden tubeless siphon)

This problem is being submitted for ETS/NTE funding as a phase 1 proposal under sorting codes for transport processing (TSE03-P) and decontamination (TSE03-Q).

This project is to study the properties of particle-laden high molecular weight polymeric solutions for applications to cleanup of contaminated solid and liquid (oil slick) surfaces. Recent experiments of Wang and Joseph [31] have shown that the addition of small solid particles in modest concentrations (<10%) to these solutions can greatly enhance the pulling power or extensional viscosity of the mixture. The research looks to the operating conditions for good cleanup, and to theoretical issues directed at understanding the extensional properties of high molecular weight polymeric solutions especially when they are laden with small particles. The methods to be employed to achieve these objectives are experimental and theoretical; theoretical issues are to be addressed also by numerical simulation and mathematical analysis.

The most compelling argument for this project is the series of click on movies of the experiments which can be found at *http://www.aem.umn.edu/research/cleanup*.

This project is associated with the remarkable properties of the tubeless siphon and particle-laden tubeless siphon which allow contaminants to be cleaned remotely by suction devices. Filaments of high molecular weight polymeric solutions can support very high extensional stresses without breaking. This allows one to siphon pools of these solutions on solid or liquid substrates remotely in a tubeless siphon. The tubeless siphon is described in standard works on rheological fluid mechanics [32, 33, 34]. The siphon may be described as follows: a fluid is sucked through a nozzle with the nozzle elevated above the surface of the liquid. Instead of the liquid breaking as in unthickened (Newtonian) liquids like water, glycerin or oil, an unsupported fluid column is drawn from a pool below into the nozzle above without breaking as shown in figures 13 and 14.

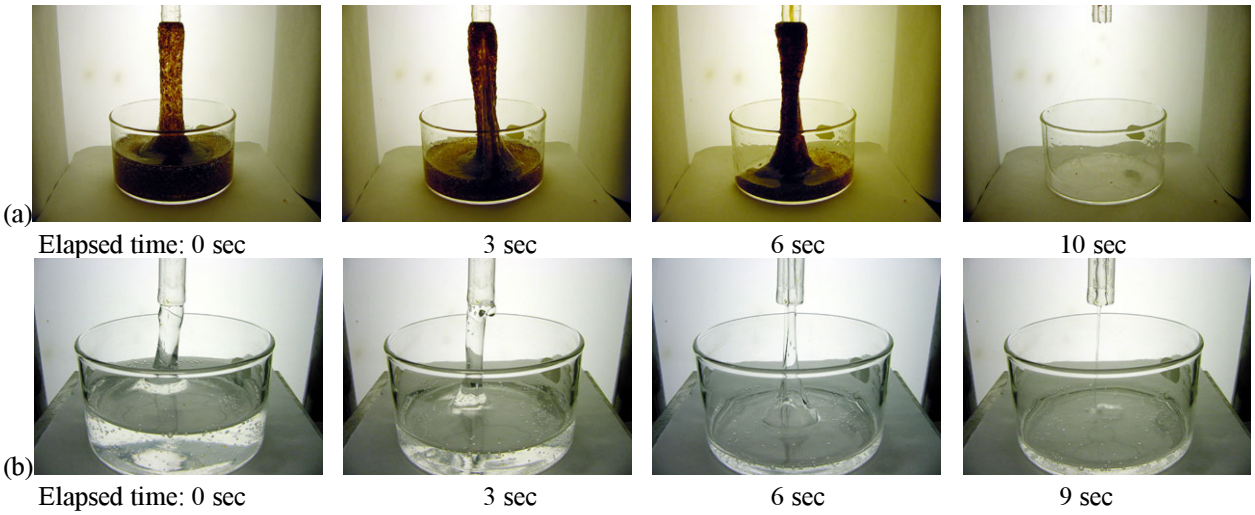

Figure 13. Sequence of photographs of a tubeless siphon of 1% aqueous Polyox at a piston speed of 0.224cm/s. (a) The siphon is loaded with about 15% by volume of 600-700 μm resin particles. All the mixture is cleaned from the beaker. (b) When there are no particles, fluid is left in the beaker. The same container is used in case (a) and (b); the initial volume of the fluid-particle mixture in (a) is equal to the initial volume of the fluid in (b).

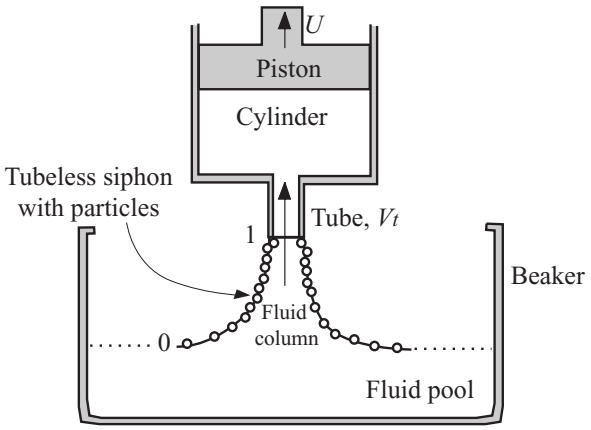

Figure 14. The schematic of the experimental set up.

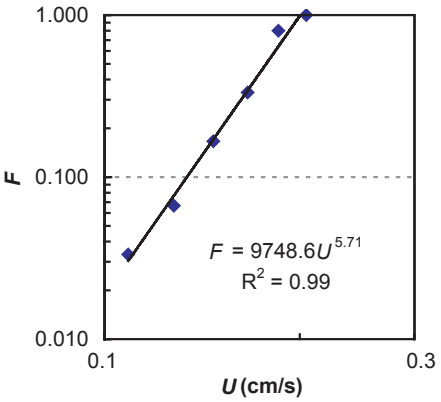

Figure 15. Suction fraction of fluid left behind as withdrawal velocity.

The thickened (viscoelastic) liquids may be sucked from a substrate remotely with a "vacuum cleaner." It appears not to have been known before the recent work of Wang and Joseph [31] that if the rate of withdrawal, the sucking power, is high enough, or if the sucking power is much lower but the liquid loaded with small particles in concentrations less than 10%, the substrate can be cleaned completely.

In the case when no particles are present, one can monitor the volume of liquid left behind after the siphon breaks as a function of the rate of suction (the velocity of the piston). The suction fraction F, defined as the volume sucked out to the initial volume, increases as 5.71 power of the velocity. At a high enough velocity one gets complete cleanup, even when no particles are present.

Similar experiments demonstrating effective cleaning by sucking off high molecular polymeric liquids were done with oil rather than water-based solvents. These experiments were motivated by the idea that if solid substrates could be cleaned by pulling off thickened liquids, preferably laden with particles, the same could be done with oil slicks. Motor oil was spread on water in a petri dish; the oil slick could not be sucked out with a handheld piston cylinder device because the oil would break when sucked. Then STP (a weakly polymeric liquid) was put on top of the motor oil and the two oils mixed. The STP-oil slick mixture could be pulled off the water easily under the same conditions that the oil alone could not be. The patent office at the University of Minnesota searched for and found a patent which had evolved to a product *Elastol*; this is a high molecular weight polymer which may be mixed with oil for oil slick removal. *Elastol* is in liquid and powder form.

Three experiments were done and can be seen at our web site or on a CD-ROM (contact *dvogel@aem.umn.edu* or see *http://www.aem.umn.edu/research/cleanup*).

1. Cleaning of solid substrates covered with oil by adding small amounts of Elastol with better cleaning when small particles are added to the oil-Elastol mixture.
2. Improved cleaning oil-slicks by adding particles to the oil-Elastol mixture.
3. Capillary attraction and self-assembly of small particles in oil slicks

These experiments will now be described with words and pictures, but they are much better described with the movies.

A handheld piston with a cylinder-sucking device is used to demonstrate the principles. There are five steps; only the three sequences showing results are shown in figures 16 and 17.

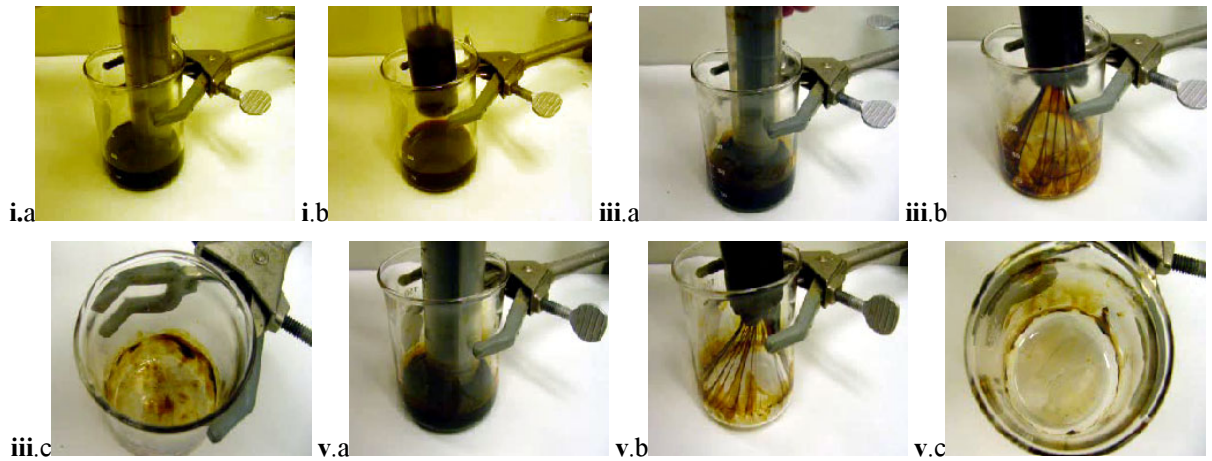

Figure 16. Cleaning oil with Elastol and Elastol plus particles. ***i****. Oil is in the beaker and it cannot be sucked out.* ***ii****. A small amount of Elastol is added to the oil (say 5%).* ***iii****. The oil plus Elastol can be pulled out but the bottom of the beaker is slightly soiled with oil.* ***iv****. Particles are added to the oil-plus-Elastol. The particles are sub-millimeter and nearly neutrally buoyant. The particles are not special, they are polydisperse and not spheres.* ***v****. The Elastol-oil-particle mixture is pulled out of the beaker; the bottom of the beaker is cleaned.*

Improved cleaning of oil slicks with particles

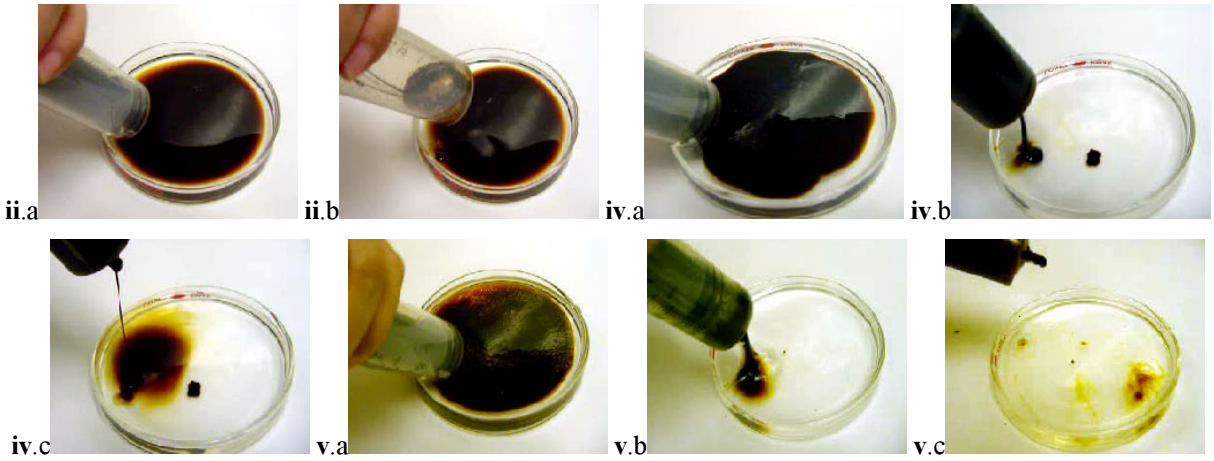

Figure 17. Oil spill remediation. ***i****. Motor oil on water in a petri dish forms an oil slick.* ***ii****. It cannot be cleaned off because the oil breaks.* ***iii****. A small amount of Elastol is added and mixes with the oil.* ***iv****. The mixture can be cleaned off, but a little slick is left.* ***v****. Particles are added. The mixture cleans up nicely, better than with no particles.*

Capillary attraction and self-assembly of small particles in oil slicks.

Heavy hydrophobic particles will float on water. They are held up by capillary forces at the contact line. When small particles are placed in an oil slick, they are covered with oil and are even more hydrophobic.

A comprehensive review of self-assembly due to capillarity can be found in [35], which has been submitted for publication and can be downloaded from *http://www.aem.umn.edu/people/faculty/joseph/archive/docs/capillarity.pdf.* The floating particles used so far in the experiments are chemically passive. The uses of active particles for remediation and decontamination have yet to be studied.

The proposed research may be applied to homeland security. The applications are to cleanup and disposal of solid and contaminated substrates. One could imagine covering a contaminated solid, a portion of an airplane or tanks, with a thickened liquid laden with particles, then sucking off the liquid,

particles and contaminant remotely with a powerful vacuum cleaner newly designed for efficient removal and disposal. The removal of particle-laden thickened liquids may be regarded as a competitor for foams say in Anthrax applications.

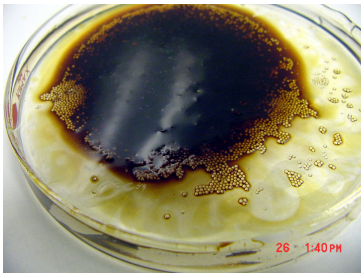

Figure 18. Capillary attraction of small particles in an oil-Elastol mixture.

If such a liquid is laid on an anthrax contaminated surface, there is no way that the spores could be aerosolized. Moreover, it is likely that the spores would be trapped in the thickened liquid and sucked away with the liquid for safe disposal. The efficient removal of oil slicks is another application, possibly more related to environmental protection than to homeland defense.

These studies aim to evaluate the effects of size, weight, concentration, wetting and reactivity properties on cleanup. What are the optimal weights and concentrations?

Suction apparatus properties

Since the cleaning property of siphon depends on the rate of withdrawal and since many requirements for effective manipulation, placement, storage and disposal will inevitably arise, the design of effective suction devices ought to be studies and implemented. Excellent results were achieved in our experiments using only a handheld piston and cylinder device. Very great improvements in cleaning can be expected from a well-designed device pointing to spreading, removal and disposal of particle-laden polymeric solutions on and from contaminated substrates.

The ***direct sciences issues*** of this research focus on understanding of particle-laden tubeless siphons under realistic conditions. The role of particles in enhancing extensional stresses is a virgin subject without prior art. The study of these topics requires understanding at a fundamental level of the mathematical modeling of viscoelastic and multiphase flow; Joseph is an expert in these two topics. Theoretical studies will be undertaken on

1. Spreading dynamics. In the vision for this kind of cleanup it would be necessary to first spread the particle-laden polymeric liquid on a contaminated substrate. Studies of spreading of viscoelastic liquids should be considered.
2. Fluid dynamics of tubeless siphons without and with particles. All of the mathematical analyses of tubeless siphons are based on idealized extensional flows which are far from reality. There is nothing in the literature on the effects of small particles on extensional flows other than the paper of Wang and Joseph [31].
3. The experiments cited in this proposal demonstrate that soiled beakers may be cleaned remotely by vacuuming the polymeric liquid at high rates of withdrawal. The study of rate effects on substrates which are not beakers needs to be understood.

The complicated problems just described are best studied by numerical methods which have been developed at Minnesota and elsewhere in successive Grand Challenge and KDI-NSF grants to D.D. Joseph, PI.

E. References

1. Singh, P. and Joseph, D.D. 2003. Floating Particles, *J. Fluid Mech.,* submitted.
2. Joseph, D.D. March 2002. *Interrogations of Direct Numerical Simulation of Solid-Liquid Flow*, eFluids.com <*http://www.efluids.com/efluids/books/joseph.htm*>, (28 December 2002).
3. Wang, J. and Joseph, D.D. 2003. Lift forces on a circular particle in Poiseuille flow of shear thinning fluids, *Phys. Fluids.*, submitted. Also available at <*http://www.aem.umn.edu/people/faculty/joseph/archive/docs/shearthinning.pdf*>.
4. Singh, P., Hesla, T.I. Joseph, D.D. 2002. Distributed Lagrange Multiplier Method for Particulate Flows with Collisions, *Int. J. Multiphase Flow*, accepted.
5. Pan, T.W., Joseph, D.D., Bai, R., Glowinski, R., Sarin, V. 2002. Fluidization of 1204 spheres: simulation and experiment, *J. Fluid Mech.*, **451**, 169-191.
6. Joseph, D.D., Ocando, D. 2002. Slip velocity and lift, *J. Fluid Mech.*, **454**, 263-286.
7. Patankar, N.A., Joseph, D.D., Wang, J., Barree, R., Conway, M., Asadi, M. 2002. Power law correlations for sediment transport in pressure driven channel flows, *Int. J. Multiphase Flow*, **28**(8), 1269-1292.
8. Wang, J., Joseph, D.D., Patankar, N.A., Conway, M., Barree, B. 2003. Bi-power law correlations for sedimentation transport in pressure driven channel flows, *Int. J. Multiphase Flow*, accepted.
9. Pan, T.-W., Glowinski, R., Joseph, D.D., Bai, R. 2002. Direct simulation of the motion of settling ellipsoids in Newtonian fluid, *14th International Conf. on Domain Decomposition Methods,* Mexico.
10. Brady, J.F. 1993. *Stokesian Dynamics Simulation of Particulate Flows in Particulate Two-Phase Flow* (M. Roco ed.) 971-998, Butterworth-Heinemann.
11. Hofler, K., Muller, M., Schwarzer, S., Wachmann, B. 1999. *Interacting particle-liquid systems, in High Performance Computing in Science and Engineering '98,* E. Krause and W. Jager eds., 54-64, Springer-Verlag, Berlin.
12. Maxey, M.R. and Patel, B.K. 1997. Force-coupled simulations of particle suspensions at zero and finite Reynolds numbers, *ASME FEDSM* 97-3188.
13. Johnson, A. and Tezduyar, T.E. 1999. Advanced mesh generation and update methods for 3D flow simulations, *Computational Mech.* **23**, 130-143.
14. Yu, Z., Tanner, R.I. and Phan-Thien, N. 2002. Direct numerical simulation of particle migration in the Couette flow. *Proceedings of 6th European conference on Rheology*, Erlangen, Germany.
15. Yu, Z., Phan-Thien, N., Fan, Y., and Tanner, R.I. 2002. Viscoelastic mobility problem of a system of particles. *J. Non-Newtonian Fluid Mech.*, **104**, 87-124.
16. Crowe, C.T., Chung, J.N., Troutt, T.R. 1996. Numerical models for two-phase turbulent flows. *Annual Review of Fluid Mechanics*, **28**, 11-43.
17. McLaughlin, J.B. 1994. Inertial computation of particle turbulent interaction. *Int. J. Multiphase Flow,* **20**, 211-232.
18. Maxey, M.R, Patel, B.K., Chang, E.J. and Wang, L.P. 1997. Simulations of dispersed turbulent multiphase flow. *Fluid Dynamics Res.*, **20**, 143-156.
19. Patankar, N.A., Ko, T., Choi, H.G., Joseph, D.D. 2001. A correlation for the lift-off of many particles in plane Poiseuille flows of Newtonian fluids, *J. Fluid Mech.*, **445**, 55-76.
20. N.A. Patankar, P.Y. Huang, T. Ko, D.D. Joseph, 2001. Lift-off of a single particle in Newtonian and viscoelastic fluids by direct numerical simulation, *J. Fluid Mech.*, **438**, 67-100.
21. Richardson, J.F. and Zaki, W.N. 1954. Sedimentation and fluidization: Part I, *Trans. Instn. Chem. Engrs.* **32**, 35–53.
22. Gerson, D.F., Zaijc, J.E. and Ouchi, M.D. 1979. *Chemistry for energy*, Ed. M. Tomlinson, ACS symposium series, 90, American Chemical Society, Washington DC, pp 66.
23. Bowden, N., Choi, I.S., Grzybowski, B.A., Whitesides, G.M. 1999. Mesoscale self-assembly of hexagonal plates using lateral capillary forces: synthesis using the "capillary bond", *J. Am. Chem. Soc*. **121**, 5373-5391.

24. Bowden, N., Terfort, A., Carbeck, J., Whitesides, G.M. 1997. Self-assembly of mesoscale objects into ordered two-dimensional arrays, *Science*, **276**, 233-235.
25. Grzybowski, B.A., Bowden, N., Arias, F., Yang, H., Whitesides, G.M. 2001. Modeling of menisci and capillary forces from the millimeter to the micrometer size range, *J. Phys. Chem. B,* **105**, 404-412.
26. Osher, S. and Sethian, J.A. 1988. Fronts propagating with curvature-dependent speed: Algorithms based on Hamilton-Jacobi formulations, *J. Comput. Phys.* **83**, 12.
27. Glowinski, R., Pan, T.-W., Hesla, T.I., Joseph, D.D. 1999. A distributed Lagrange multiplier/fictitious domain method for particulate flows, *Int. J. Multiphase Flows* **25**(5), 755.
28. Poynting, J.H. and Thompson, J.J. 1913. *A Text-book of Physics: Vol. 1, Properties of Matter*, C. Griffith & Co. Ltd, London, p. 153-155.
29. Gibbs, J.W. 1906. *The Scientific Papers of J. Willard Gibbs, Vol. I: Thermodynamics*. Longmans Green & Co. (Dover Reprint, 1961).
30. Oliver, J.F. Hu, C., Mason, S.G. 1976. Resistance to spreading of liquids by sharp edges. *J. Colloid Interface Science*, **59**, 568-581.
31. Wang, J., Joseph, D.D. 2003. Particle-laden tubeless siphon, *J. Fluid Mech*. accepted.
32. Bird, R. B., Armstrong, R. C. and O. Hassager, 1977, 1987. *Dynamics of Polymeric Liquids, Volume 1, Fluid Mechanics*, Wiley, New York.
33. Joseph, D.D. 1990. *Fluid Dynamics of Viscoelastic Liquids.* Springer Applied Math Series.
34. Macosko, C.W. 1994, *Rheology: Principles, Measurements, and Applications*, Wiley-VCH.
35. Joseph, D.D., Wang, J., Bai, R. Yang, B.H., Hu, H. 2002. Particle motion in a liquid film rimming the inside of a partially filled rotating cylinder, *J. Fluid Mech.*, submitted.